

Chiral phase properties of finite size quark droplets in the Nambu–Jona-Lasinio model

O. Kiriya^{*} and A. Hosaka[†]

Research Center for Nuclear Physics, Osaka University, Ibaraki 567-0047, Japan

(Dated: January 29, 2020)

Chiral phase properties of finite size hadronic systems are investigated within the Nambu–Jona-Lasinio model. Finite size effects are taken into account by making use of the multiple reflection expansion. We find that, for droplets with relatively small baryon numbers, chiral symmetry restoration is enhanced by the finite size effects. However the radius of the stable droplet does not change much, as compared to that without the multiple reflection expansion.

PACS numbers: 11.30.Rd, 12.38.Lg, 12.39.-x

I. INTRODUCTION

The behavior of (finite lumps of) quark matter is of great interests in cosmology, neutron stars, cosmic ray physics and heavy ion collisions [1, 2]. Absolutely stable nonstrange quark matter contradicts ordinary nuclei consisting of neutrons and protons. However, the existence of stable strange quark matter is still an open question and it may be realized in the form of strangelets, small lumps of strange quark matter. The (meta)stability of nonstrange and strange quark matter has been investigated within the MIT bag model [3], quark mass density dependent model [4], Nambu–Jona-Lasinio (NJL) model [5], and so on [6]. In the MIT bag model, which assumes that asymptotically free quarks are confined in a bag, the bag constant and the current quark masses are phenomenological input parameters. Farhi and Jaffe [7] found a reasonable range of these parameters in which strange quark matter is stable, while nonstrange quark matter is unstable as compared to a gas of ^{56}Fe . The quark mass density dependent model takes account of the confinement mechanism by introducing density dependent quark masses. Fowler *et al.* [4] concluded that the critical density for a phase transition between nuclear and quark matter is sensitively dependent on the confinement mechanism. In the NJL model, the bag constant and constituent quark masses are generated dynamically in marked contrast to the above mentioned models. In Ref. [8], it has been argued that stable nonstrange quark matter lies in chirally restored phase and, then, the model shows similar behavior to the MIT bag model (see, also, Ref. [9]). The stability of strange quark matter has been also studied and concluded that strange quark matter is not absolutely stable when realistic values of current quark masses and coupling constants are used [10].

On the other hand, unlike bulk systems, finite size effects cannot be ignored in the study of finite lumps of quark matter. So far, the MIT bag model and Fermi gas model including finite size effects have been widely used to study their properties [7, 11, 12, 13, 14, 15]. For finite quark matter, it is known that the lumps are not energetically favored by finite size effects. The disfavor also arises from large strange quark masses. Therefore, finite size effects on dynamical quark masses (i.e. the behavior of chiral symmetry) might have significant effects on their properties. In this paper, we adopt the NJL model that is a simple tractable model respecting chiral symmetry. Then we consider isospin symmetric ($n_u = n_d$ with $n_i = \langle q_i^\dagger q_i \rangle$) quark droplets. Finite size effects are taken account of by making use of the multiple reflection expansion (MRE) [11, 14, 16] which is an approximation for the density of states in finite systems. The MRE itself has been derived for free massless particles or nonrelativistic particles. However, the MRE has been used to calculate the thermodynamic quantities of *massive* quarks and reproduced well the results of the MIT bag model [2, 11, 14, 15]. We expect that it also works well in the NJL model with the mean field approximation and apply the MRE to the effective potential of the model.

^{*}Electronic address: kiriya@rcnp.osaka-u.ac.jp

[†]Electronic address: hosaka@rcnp.osaka-u.ac.jp

This paper is organized as follows. In Sec. II, we formulate the effective potential of spherical quark droplets that consist of an equal number of up and down quarks. The Schwinger–Dyson equation and related thermodynamic quantities are also derived. In Sec. III, we present numerical results. Section IV is devoted to conclusions.

II. THE MODEL

In this section, the effective potential and related thermodynamic quantities of spherical quark droplets are derived in the two-flavor NJL model. We consider up and down quarks to be massless. Then, the $SU(2)_L \times SU(2)_R$ chirally symmetric Lagrangian is given by

$$\mathcal{L} = \bar{\psi} i \gamma^\mu \partial_\mu \psi + G [(\bar{\psi}\psi)^2 + (\bar{\psi} i \gamma_5 \vec{\tau} \psi)^2], \quad (1)$$

which is our starting point. Here, ψ denotes a quark field with two flavors ($N_f = 2$) and three colors ($N_c = 3$), and G is a dimensionful coupling constant (mass^{-2}). The Pauli matrices $\vec{\tau}$ act in the flavor space.

Let us first discuss the effective potential for bulk systems. In the mean-field (Hartree) approximation, the effective potential ω at finite temperature T and quark chemical potential μ is written as [5]

$$\omega = \frac{m^2}{4G} - \nu \int \frac{k^2 dk}{2\pi^2} E_k - \nu T \int \frac{k^2 dk}{2\pi^2} \ln \left[1 + e^{-\beta(E_k + \mu)} \right] \left[1 + e^{-\beta(E_k - \mu)} \right], \quad (2)$$

where $\nu = 2N_f N_c$, $E_k = \sqrt{k^2 + m^2}$, $\beta = 1/T$, with m being the dynamically generated (constituent) quark mass. Since the model is not renormalizable, we have to specify a regularization scheme. Throughout this paper, we use a sharp cutoff $\Lambda = 600$ MeV in the three dimensional momentum space with the coupling constant $G\Lambda^2 = 2.45$ [8]. With these parameters, the vacuum values of the pion decay constant f_π , the constituent quark mass m and the quark condensate are obtained as $f_\pi = 93.9$ MeV, $m = 400$ MeV and $\langle \bar{u}u \rangle = \langle \bar{d}d \rangle = (-244.9 \text{ MeV})^3$. Further discussions about the stability of nonstrange quark matter can be found in Refs. [8, 9].

We now turn to discussions on finite size droplets. Within the framework of the MRE [11, 14, 16], we write the density of states for a spherical system as $k^2 \rho_{\text{MRE}}/(2\pi^2)$, where

$$\rho_{\text{MRE}} = \rho_{\text{MRE}}(k, m, R) = 1 + \frac{6\pi^2}{kR} f_S \left(\frac{k}{m} \right) + \frac{12\pi^2}{(kR)^2} f_C \left(\frac{k}{m} \right), \quad (3)$$

with R being the radius of the sphere. The functions $f_S(k/m)$ and $f_C(k/m)$ represent the surface and the curvature contributions to the fermionic density of states, respectively. The functional form of the surface contribution is given by

$$f_S \left(\frac{k}{m} \right) = -\frac{1}{8\pi} \left(1 - \frac{2}{\pi} \arctan \frac{k}{m} \right). \quad (4)$$

On the other hand, the curvature contribution for an arbitrary quark mass has not been derived in the MRE. In this paper, we adopt the following *Ansatz* by Madsen [14]:

$$f_C \left(\frac{k}{m} \right) = \frac{1}{12\pi^2} \left[1 - \frac{3k}{2m} \left(\frac{\pi}{2} - \arctan \frac{k}{m} \right) \right]. \quad (5)$$

Note that Eqs. (4) and (5) have the following $m \rightarrow 0$ limits:

$$\lim_{m \rightarrow 0} f_S(k/m) = 0, \quad \lim_{m \rightarrow 0} f_C(k/m) = \frac{-1}{24\pi^2}. \quad (6)$$

Thus, the effective potential for the spherical system is given by

$$\omega = \frac{m^2}{4G} - \nu \int_0^\Lambda \frac{k^2 dk}{2\pi^2} \rho_{\text{MRE}} E_k - \nu T \int_0^\Lambda \frac{k^2 dk}{2\pi^2} \rho_{\text{MRE}} \ln \left[1 + e^{-\beta(E_k + \mu)} \right] \left[1 + e^{-\beta(E_k - \mu)} \right]. \quad (7)$$

Henceforth we restrict ourselves to zero temperature. For computation of a finite system, we choose a fixed baryon number A and a radius of the sphere R . The quark mass m is then determined by the Schwinger–Dyson equation (SDE) that is the extremum condition of ω with respect to m . In terms of the Fermi momentum k_F , the SDE is obtained as

$$m = 2G\nu \frac{\partial}{\partial m} \int_{k_F}^{\Lambda} \frac{k^2 dk}{2\pi^2} \rho_{\text{MRE}} E_k + 2G\nu \sqrt{k_F^2 + m^2} \frac{\partial}{\partial m} \int_0^{k_F} \frac{k^2 dk}{2\pi^2} \rho_{\text{MRE}}, \quad (8)$$

where the Fermi momentum is related to the chemical potential by $\mu = \sqrt{k_F^2 + m^2}$. In addition to the SDE, since the baryon number is fixed to A , we have another equation, i.e.

$$V n_B = V \frac{\nu}{3} \int_0^{k_F} \frac{k^2 dk}{2\pi^2} \rho_{\text{MRE}} = A, \quad (9)$$

where $V = 4\pi R^3/3$ is the volume of the droplet and n_B denotes the baryon number density in the droplet that is one third of the quark number density n_q :

$$n_B = \frac{n_q}{3} = -\frac{1}{3} \left(\frac{\partial \omega}{\partial \mu} \right)_T \rightarrow \frac{\nu}{3} \int_0^{k_F} \frac{k^2 dk}{2\pi^2} \rho_{\text{MRE}} \quad (10)$$

as $T \rightarrow 0$. Equations (8) and (9) have to be solved self-consistently. Therefore, by virtue of Eq. (9), one can reduce these equations to the following set of coupled equations:

$$m = 2G\nu \frac{\partial}{\partial m} \int_{k_F}^{\Lambda} \frac{k^2 dk}{2\pi^2} \rho_{\text{MRE}} E_k, \quad (11)$$

$$V \frac{\nu}{3} \int_0^{k_F} \frac{k^2 dk}{2\pi^2} \rho_{\text{MRE}} = A. \quad (12)$$

Once we know the density dependent (i.e. the radius dependent) quark mass m , the pressure p and the energy density ϵ inside the droplet are given by

$$p = \nu \int_{k_F}^{\Lambda} \frac{k^2 dk}{2\pi^2} \rho_{\text{MRE}} E_k + \frac{3A}{V} \sqrt{k_F^2 + m^2} - \frac{m^2}{4G}, \quad (13)$$

$$\epsilon = -\nu \int_{k_F}^{\Lambda} \frac{k^2 dk}{2\pi^2} \rho_{\text{MRE}} E_k + \frac{m^2}{4G}. \quad (14)$$

We note that, unlike the bulk case, the SDE (11) does not have a trivial solution $m = 0$. The reason is that ρ_{MRE} , the density of states of the MRE, depends on the quark mass m , and hence the r.h.s. of the SDE (11) is no longer proportional to m , in contrast to the bulk case.

III. NUMERICAL RESULTS

In this section, we present the numerical results. Unless stated otherwise, the baryon number A is fixed to $A = 100$.

For a given baryon number, a nontrivial solution to the coupled equations (11) and (12) is obtained as a function of the radius R . Then, as shown in Fig. 1, the pressure of chirally symmetric and broken phases are calculated from Eq. (13). As a result, the critical radius at which the chiral phase transition occurs is identified as $R_c^{(\text{MRE})} \simeq 12$ fm. The corresponding critical baryon number density $n_c^{(\text{MRE})}$ is rather small $n_c^{(\text{MRE})} \simeq 0.08n_0$ with n_0 being normal nuclear matter density $n_0 = 0.17$ fm⁻³. [22]

The resultant quark mass as a function of the radius is shown in Fig. 2. Since the baryon number is fixed, by changing the radius R , the baryon number density n_B changes. Therefore, Fig. 2 implies that the phase transition as n_B is varied is of first-order when the effect of the MRE is included. For comparison, we also present the result without the MRE showing that the transition at $R_c \simeq 4$ fm is of second-order. The difference between these two curves obviously stems from the finite size effects. This result is roughly interpreted as follows. In the MRE, the finite size effects reduce the density of

states and, therefore, the *actual* Fermi momentum increases for a given baryon number. The increasing tendency of the Fermi momentum is more pronounced when the baryon number is small (see Fig. 3). As a consequence, the chirally broken phase is energetically disfavored for small baryon numbers.

Figure 4 shows the quark mass as a function of the radius for the cases of $A = 100$ and $A = 1000$. It is clear that, for relatively large baryon numbers, the first-order transition is weakened. In addition, at $A = 1000$ we find $R_c^{(\text{MRE})} \simeq 14$ fm and $n_c^{(\text{MRE})} \simeq 0.5n_0$. These results, of course, indicate that the finite size effects become less important for large baryon numbers.

Let us consider the radius of the stable droplet from the usual pressure balance relation between the inside of the droplet and the vacuum (the outside of the droplet). The pressure inside the droplet with and without the MRE are shown in Fig. 5 for $A = 100$, where the vacuum pressure is taken to be zero. When R is small, the pressures are positive and chiral symmetry is restored inside the droplet. As R is increased the pressures decrease. Now without the finite size effects (MRE) the pressure keeps decreasing in the negative pressure region toward the cusp point, where the chiral phase transition takes place. Beyond the cusp point, the pressure curve follows the one in the chirally broken phase and turns into the positive region (but with small values), asymptotically approaching the zero value. There are two points where the pressure curve passes the zero, where the system is in equilibrium. The left point ($R \simeq 3.7$ fm) corresponds to the absolute minimum of the energy per baryon, while the right point ($R \simeq 7.5$ fm) corresponds to the local maximum. Consequently, the stable droplet of radius $R_s \simeq 3.7$ fm lies in the chirally symmetric phase.

On the other hand, with the MRE the pressure crosses zero only at $R \simeq 3.5$ fm. We have calculated the pressure up to $R = 10^8$ fm and confirmed that the pressure of the chirally broken phase is always negative. Therefore, we find $R_s^{(\text{MRE})} \simeq 3.5$ fm, which is somewhat small as compared to that without the MRE, and the stable droplet lies in the chirally symmetric phase. The radius of a stable droplet is presented in Fig. 6 as a function of A . As is evident from the figure, as long as A is sufficiently large, $R_s^{(\text{MRE})}$ varies as $A^{1/3}$. This result implies that, as mentioned before, the finite size effects are less important at large baryon numbers. Incidentally, we have observed the saturation property ($R \sim A^{1/3}$) when A is large. This is a consequence of the balance between the kinetic energy of quarks and the (bag like) volume type potential energy.

IV. CONCLUSIONS

We have studied the behavior of chiral symmetry in finite systems within the $SU(2)_L \times SU(2)_R$ symmetric Nambu–Jona-Lasinio model. The multiple reflection expansion was used to take account of finite size effects. We considered spherical quark droplets with baryon numbers $A = 100 - 1000$. The Schwinger–Dyson equation for the quark mass was solved and, then, it turned out that the finite size effects enhance chiral symmetry restoration. The critical radii with and without the MRE differed significantly from each other. If the finite size effects are important also for strange quarks, it may have significant effects on the (meta)stability of strangelets. On one hand, the enhancement of restoring chiral symmetry lowers the constituent mass of strange quarks. This affects the argument made by Buballa and Oertel [10] who pointed out that the large strange quark mass at the relevant densities is the main reason that makes strange quark matter unstable. On the other hand, the finite size effects increase the energy of strangelets [2, 11, 14, 15]. These two competing aspects should be carefully treated in realistic calculations

In order to find the radius of the stable droplet, we calculated the pressure inside the droplet. Without the finite size effects (MRE) the pressure shows the characteristic behavior as shown in Fig. 5. Such behavior has been also obtained [9, 17] with interactions/parameters which differ from those in this paper. In contrast, with the MRE its behavior changes considerably. We found that the pressure of the chirally broken phase is always negative and, therefore, the chirally broken phase is unstable against collapse. However, the radius of the stable droplet does not change much as compared to that without the MRE. After all, it was found that chiral symmetry is restored in the stable droplet. This result reminiscent of the MIT bag model supports the former results without the MRE [8, 9].

We have already referred to the validity of the MRE in the first section. It should be also noted that the MRE contains several problems concerning its reliability. In the first place, ρ_{MRE} should have terms proportional to $1/R^3$, $1/R^4$, and so on, though their functional forms are not known. These terms would be dominant at small radii. Furthermore, it is well known that the MRE causes unphysical negative density of states at small radii. Neergaard and Madsen [18] have investigated the validity of the MRE

and proposed a solution to these problems. However, for systems of $A \gtrsim 50$, these problems have rather minor effects and the results presented here should hold when improved density of states is employed.

Finally, we comment on the outlook for future studies. Physics of strangelets and the quark droplets at finite temperature should have important implications for the cosmological quark-hadron phase transition and heavy ion collision experiments. It is worthwhile doing more detailed analysis including charge neutrality, chemical equilibrium by weak interactions and the color singlet constraint. Furthermore, it is also interesting to include other dynamical effects as well as the chiral phase transition, e.g., color superconductivity and color flavor locking [19, 20, 21]. They may alter the present phase structure at small radii, because, at sufficiently low temperatures and high densities, the chirally broken phase would undergo a phase transition into the color superconducting phase.

Acknowledgments

We are grateful to S. Raha for suggesting this subject and for stimulating discussions. We also thank to N. Sandulescu and S. Yasui for valuable discussions.

-
- [1] A. R. Bodmer, Phys. Rev. D **4**, 1601 (1971); E. Witten, Phys. Rev. D **30**, 272 (1984).
 - [2] See, for example, *Proceedings of the International Symposium on Strangeness in Quark Matter*, Santorini, 1997, J. Phys. G **23**, No. 12 (1997); J. Madsen, in *Proceedings of the Eleventh Chris Engelbrecht Summer School*, Capetown, South Africa, 1998, edited by J. Cleymans *et al.* (Springer-Verlag, Berlin, 1999), and the references cited therein.
 - [3] A. Chodos, R. L. Jaffe, K. Johnson, and C. B. Thorn, Phys. Rev. D **9**, 3472 (1974).
 - [4] G. N. Fowler, S. Raha, and R. M. Weiner, Z. Phys. C **9**, 271 (1981).
 - [5] For reviews, see U. Vogl and W. Weise, Prog. Part. Nucl. Phys. **27**, 91 (1991); S. P. Klevansky, Rev. Mod. Phys. **64**, 649 (1992); T. Hastuda and T. Kunihiro, Phys. Rep. **247**, 241 (1994).
 - [6] K. Schertler, C. Greiner, and M. H. Thoma, J. Phys. G **23**, 2051 (1997); W. M. Alberico, A. Drago, and C. Ratti, Nucl Phys. **A706**, 143 (2002).
 - [7] E. Farhi and R. L. Jaffe, Phys. Rev. D **30**, 2379 (1984).
 - [8] M. Buballa, Nucl. Phys. **A611**, 393 (1996).
 - [9] M. Alford, K. Rajagopal, and F. Wilczek, Phys. Lett. B **422**, 247 (1998).
 - [10] M. Buballa and M. Oertel, Phys. Lett. B **457**, 261 (1999); I. N. Mishustin, L. M. Satarov, H. Stöcker, and W. Greiner, Phys. Atom. Nucl. **64**, 802 (2001).
 - [11] M. S. Berger and R. L. Jaffe, Phys. Rev. C **35**, 213 (1987); **44**, 566(E) (1991).
 - [12] D. Vasak, W. Greiner, and L. Neise, Phys. Rev. C **34**, 1307 (1986).
 - [13] C. Greiner, D. H. Rischke, H. Stöcker, and P. Koch, Phys. Rev. D **38**, 2797 (1988).
 - [14] J. Madsen, Phys. Rev. Lett. **70**, 391 (1993); Phys. Rev. D **47**, 5156 (1993); **50**, 3328 (1994).
 - [15] E. P. Gilson and R. L. Jaffe, Phys. Rev. Lett. **71**, 332 (1993).
 - [16] R. Balian and C. Bloch, Ann. Phys. **60**, 401 (1970).
 - [17] T. M. Schwarz, S. P. Klevansky, and G. Papp, Phys. Rev. C **60**, 055205 (1999).
 - [18] G. Neergaard and J. Madsen, Phys. Rev. D **60**, 054011 (1999); **62**, 034005 (2000).
 - [19] See, for example, K. Rajagopal and F. Wilczek, in *At the Frontier of Particle Physics – Handbook of QCD: Boris Ioffe Festschrift*, edited by M. Shifman (World Scientific, Singapore, 2001); M. Alford, Ann. Rev. Nucl. Part. Sci. **51**, 131 (2001).
 - [20] J. Madsen, Phys. Rev. Lett. **87**, 172003 (2001).
 - [21] P. Amore, M. C. Birse, J. A. McGovern, and R. Walet, Phys. Rev. D **65**, 074005 (2002).
 - [22] In the case of bulk matter, our model parameters yield the critical density $n_c^{(QM)} \simeq 2n_0$.

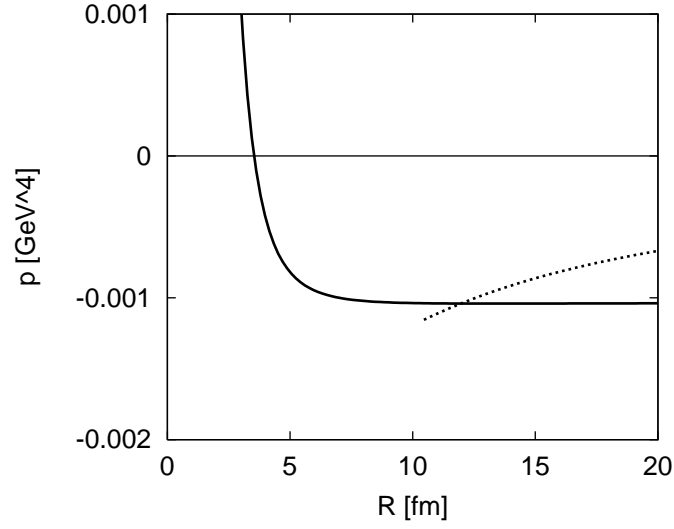


FIG. 1: The pressure inside a droplet as a function of R for $A = 100$. The solid line shows the pressure of chirally symmetric phase and the dotted line shows that of chirally broken phase. Two lines cross at $R \simeq 12$ fm. Notice that the vacuum (the outside of the droplet) pressure is taken to be zero.

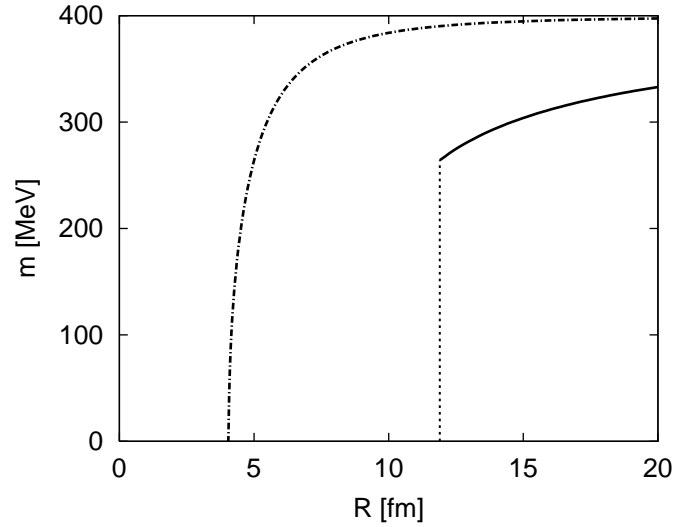


FIG. 2: Radius dependence of the quark mass for $A = 100$ (solid line). For comparison, the result without the MRE is presented by dot-dashed line.

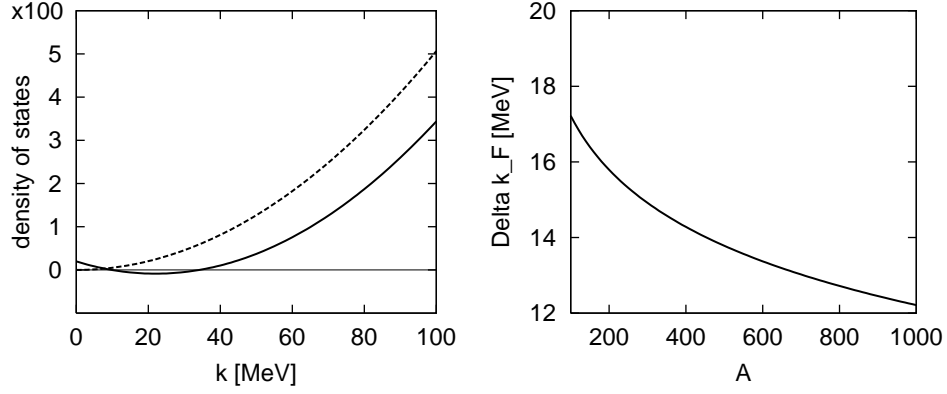


FIG. 3: The density of states $k^2 \rho_{\text{MRE}} / (2\pi^2)$ (solid line) and that without the MRE (dotted line) in unit of MeV^2 as a function of k (left panel). The increase of the Fermi momentum due to the finite size effects Δk_F as a function of A (right panel). The quark mass m and the radius R are taken to be their typical values; $m = 200$ MeV and $R = 10$ fm.

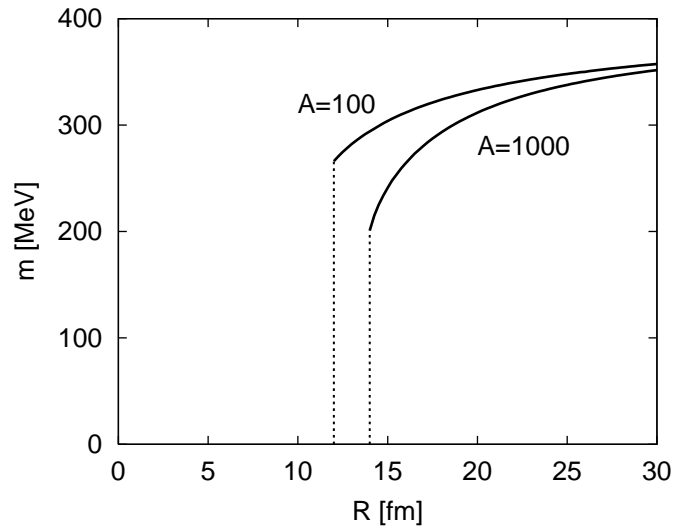


FIG. 4: The radius dependence of the quark mass for the cases of $A = 100$ and $A = 1000$. For relatively large baryon number, the first-order transition is weakened.

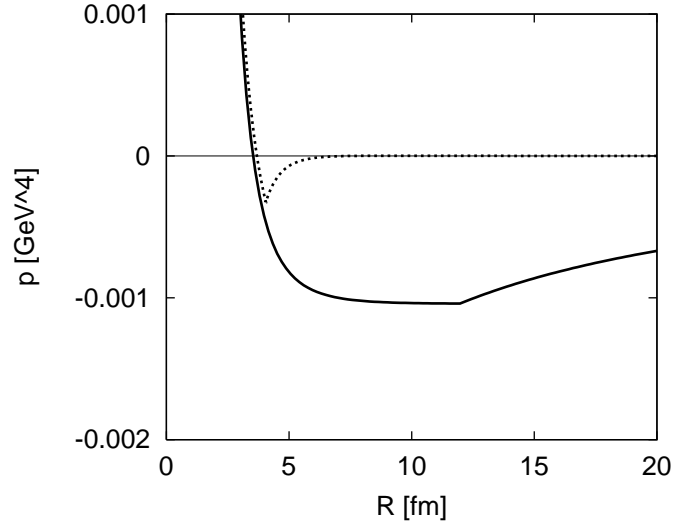


FIG. 5: The pressure inside a droplet ($A = 100$) as a function of R . The curves correspond to the pressure with (solid line) and without (dotted line) the MRE. Without the MRE the pressure becomes positive for $R \gtrsim 7.5$ fm, though it is difficult to see in this figure.

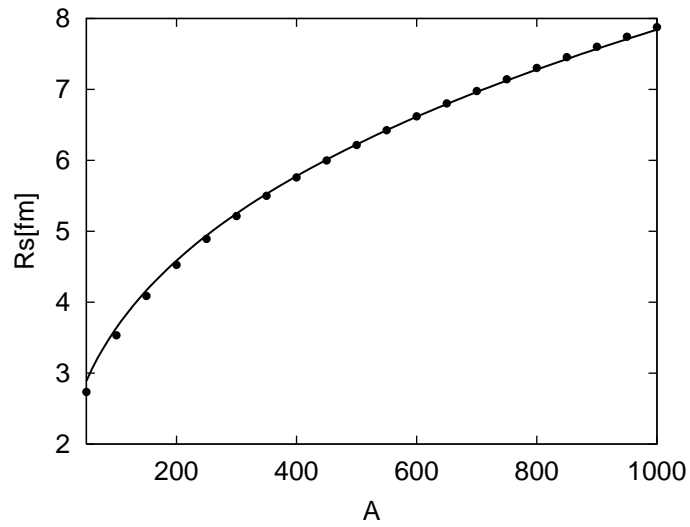


FIG. 6: The radius of the stable droplet $R_s^{(\text{MRE})}$ as a function of baryon number (blobs). The solid line shows χ^2 fitting to $R_s^{(\text{MRE})} \propto A^{1/3}$.